

## Gas Hydrate occurrences in the Andaman offshore, India – Seismic Inferences

N. Satyavani\*, Kalachand Sain and V. Jyothi

CSIR-National Geophysical Research Institute, Uppal Road, Hyderabad - 500007

\*Corresponding author: satyavani\_nittala@yahoo.com

---

### ABSTRACT

Multi-Channel Seismic (MCS) data in Andaman offshore shows a prominent bottom simulating reflector (BSR) at a depth of ~575 meters below the seafloor (mbsf), indicating the presence of gas hydrates/free gas in the region. Based on AVO modeling and attenuation ( $Q^{-1}$ ), an attempt has been made to qualify if the BSR is related to gas-hydrates underlain by free gas. The travel time tomography of identifiable seismic phases has also been carried out to delineate the general distribution of gas hydrates and/or free gas along the seismic line. The increase in seismic amplitudes at BSR, almost double to that of the seafloor, indicates the presence of free gas below the BSR and the study of  $Q$  made at two locations (with and without BSR) indicates the presence of gas hydrates above the BSR. These observations are further confirmed by the results of travel time tomography where a ~200m free gas zone with a velocity of 1.4-1.7km/s is found to be overlain by ~400m thick gas hydrate zone with a velocity of 1.8-2.2km/s.

---

### INTRODUCTION

The presence of gas hydrates is usually inferred by seismic experiment by identifying an anomalous reflector, known as the bottom simulating reflector (BSR) on the seismic section. Basically, the BSR is an interface between gas hydrate-bearing sediments above and free gas zone below. The presence of gas hydrate in the sediments increases the rigidity of the sediments and thereby increases seismic velocity ( $V_p$ ), while presence of free-gas beneath the BSR appreciably reduces the seismic velocity and produces velocity reversal across the interface.

The seismic data in the Andaman offshore shows a clear BSR at a depth of ~575 m below seafloor (mbsf), that predominantly cross-cuts the local stratigraphy and is associated with negative polarity. The unusual depth of BSR has raised doubts about its association with gas hydrates and needed further research to ascertain the presence of gas hydrates. The computation of seismic attributes from surface seismic data has demonstrated that BSR is due to gas hydrates underlain by free gas (Satyavani et al., 2008), which was corroborated further by drilling and coring of Indian National Gas Hydrate Program (Collett et al., 2008). In the present study, we attempt to characterize the gas hydrates/free-gas bearing sediments using seismic data, through amplitude versus offset (AVO) patterns, followed by seismic attenuation studies to provide the evidence of gas hydrates. In addition, we have derived a velocity-depth section along the seismic line by employing the ray-based travel time modeling. The AVO studies show free gas below the BSR, while seismic attenuation provides evidence for the presence of gas hydrates above the BSR. The results are

in agreement with the inferences drawn from the drilling. Further, velocity modeling has brought out a low-velocity free gas zones overlain by a high velocity gas hydrates layer.

### STUDY AREA

The Andaman basin, located in the southeastern part of the Bay of Bengal is a portion of large geotectonic unit that extends from Indonesian Islands in the south to Myanmar in the north. The Andaman basin is believed to have formed due to initiation of spreading activity in the Central Andaman Trough (Raju et al., 2004). The principal source of the sediment for the evolution of the hydrocarbon system comes from the Irrawaddy River flowing in Burma, which is the main source of sediments flowing into the Andaman basin (Wandrey, 2006). The basin is marked by prominent morphological features such as the Narcondam Deep, Invisible Bank, Fore-Arc basin and consists of several faults, grabens and seamounts (Fig.1).

The spatial distribution of discovered hydrocarbons within the Sumatra-Andaman-Myanmar belt indicates that the Andaman basin might host substantial gas reserves. The hydrocarbon potential is mainly controlled by the source rock deposition in the area (Krishnamohan et al., 2006). The present study area lies between the Andaman trench and the volcanic arc associated with the subduction zones. Biogenic gas (mainly methane) related to the sediment accretion in the subduction zones is believed to aid the formation of gas hydrates (Chopra, 1985). The favorable water depth, rapid sedimentation, mature organic matter, various types of faults indicate good prospects of gas hydrates in the Andaman fore-arc region.

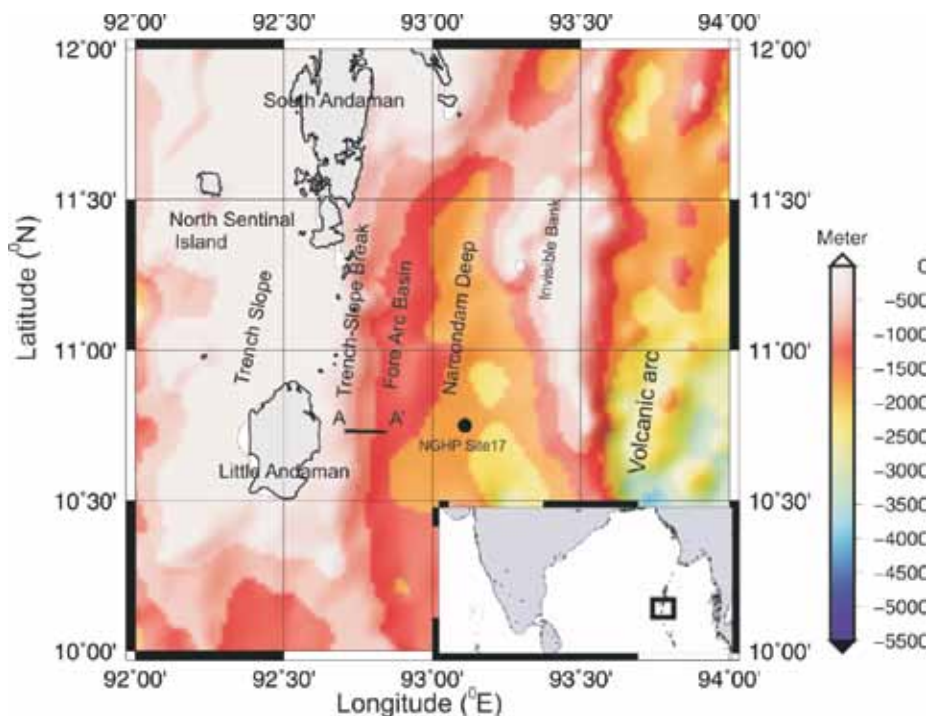


**Figure 1.** The map of the Andaman offshore region showing the multi-channel seismic line and the bathymetry. Solid circle shows the drill location of NGHP-01 Expedition.

**SEISMIC DATA**

The seismic data used for this study was collected by Oil and Natural Gas Corporation (ONGC) in 1999 by a 384 channel streamer with a GI gun of 2,250 cubic inches as the seismic source. The shot and receiver intervals are 25m and 12.5 m respectively, resulting in 96 fold multi-channel seismic data. The near trace offset is 206 m, and the far offset is 4,987.5 m. The pre-processing steps include, band pass filtering (8-10-80-90 Hz); true amplitude recovery (6db/s); predictive deconvolution (2 ms prediction distance and operator length of 160 ms). The velocity analysis is carried out in two passes. In the first pass, the velocity picking is done at every 2 km interval, while in the second pass we pick the velocities at every 1 km, using the earlier velocity as starting model. A very closely spaced (1 km) velocity analysis is thus carried out in 2 iterations and a smoothed velocity field is obtained. Normal move out correction (NMO) is applied using this velocity field, with a stretch mute of 30% and the data are then stacked. In the post stack processing stage, we used FX deconvolution to improve upon the continuity of the reflectors. A post-stack Memory Stolt migration is carried out to improve the image. The resulting stack section along the seismic line is shown in Fig. 2.

The seismic image shows the complex patterns of the sub-sea stratigraphy with highly folded and faulted structures. A very prominent reflector, cross-cutting the stratigraphic boundaries and showing a negative polarity

compared to the seafloor is identified as BSR. This reflector is nearly parallel to the seafloor and polarity reversal can be noticed between CDP 551 and 991, occurring at a two-way time (TWT) of ~2,500 ms, or ~ 640 ms below the seafloor. The depth to this reflector from the seafloor is about 575 mbsf (Fig.2). A representative seismic gather at CDP 536 is shown in Fig. 3, where the seafloor is noticed at ~1,860 ms, and the BSR is observed at 2,500 ms.

**AVO STUDIES**

The reflection from BSR exhibits pronounced amplitude increase with offset (Fig.3) and this AVO pattern indicates the presence of free gas below the BSR. The AVO study has been effectively used as a tool for identifying gas hydrates (Hyndman and Spence, 1992; Andreassen et al., 1997; Ecker et al., 1998; Yuan et al., 1999). In some cases, there is also a phase shift observed on AVO, which represents the turning rays within the high velocity hydrate layer above the BSR (Hyndmann and Spence, 1992). The AVO data is usually extracted from the MCS data (Shot / CDP gathers) and is capable of providing the information about the compressional (P-wave) and shear (S-wave) wave velocities of the sediment. The occurrence of gas hydrate in sediment increases both the P- and S-wave velocities but the presence of free gas significantly lowers the P-wave velocity without much influence on the S-wave velocity. The seismic reflection from the BSR exhibits a wide range of AVO patterns depending on the saturation of gas

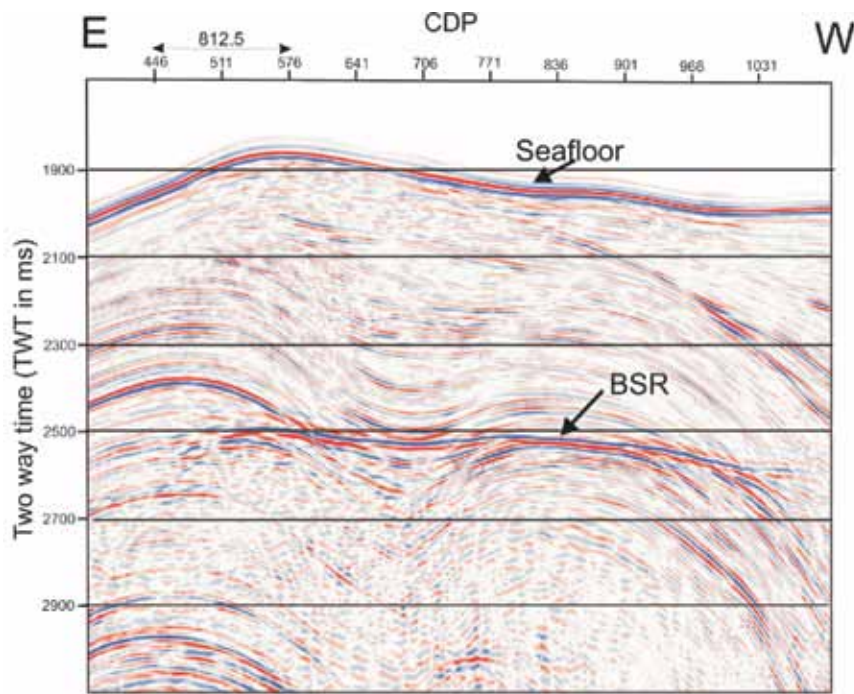


Figure 2. The seismic stack section along the MCS line.

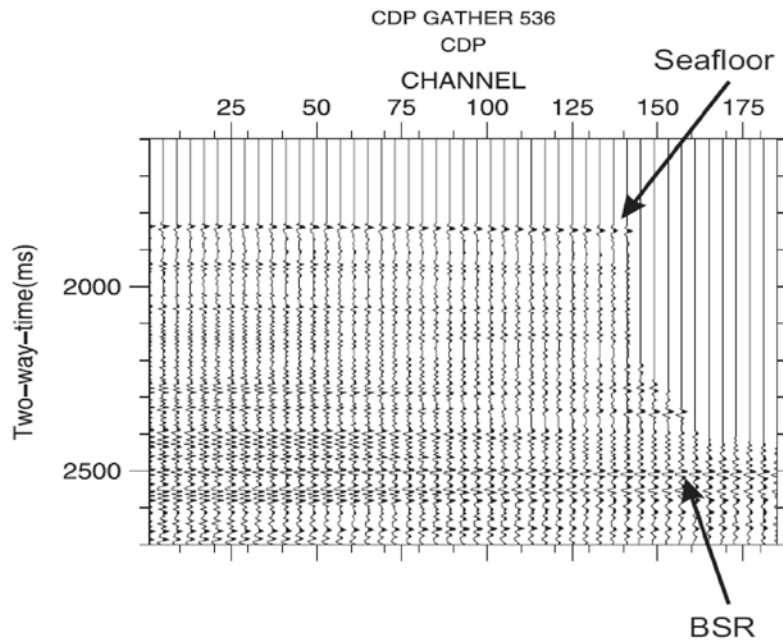
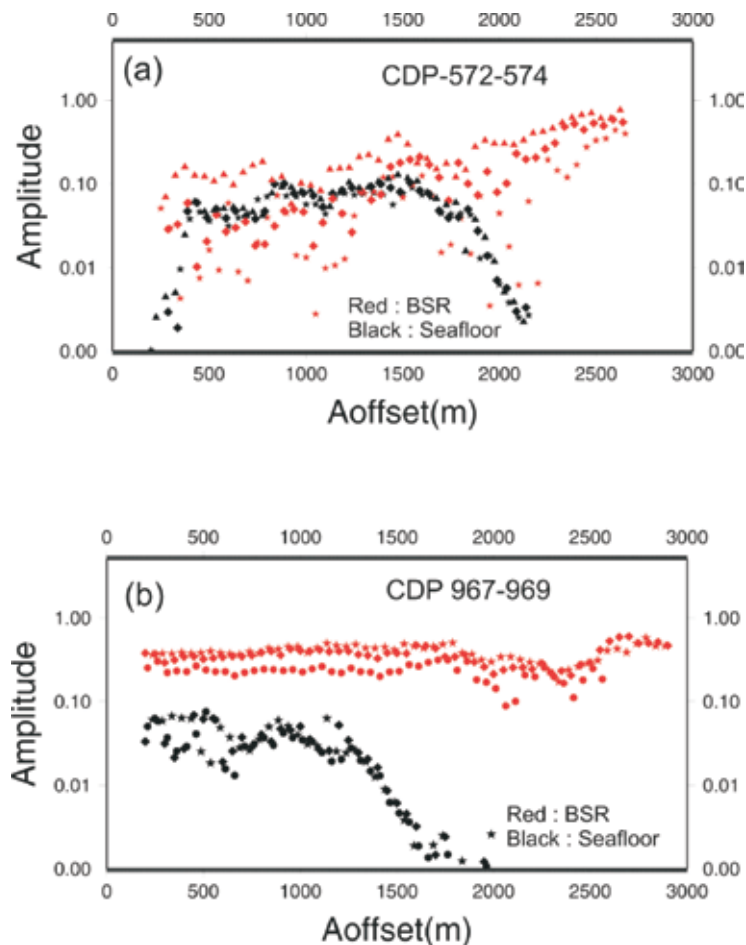


Figure 3. Shot gather CDP536 showing a clear increase in seismic amplitude with offset.

hydrates and their distribution above the BSR. This also depends on the nature of distribution of free gas below the BSR. In this study, we present only the qualitative aspect of AVO studies by incorporating the effect of source and receiver directivity in visualizing the seismic amplitudes. Here, an attempt has been made to investigate the AVO

character of the BSR by taking a group of CDPs with and without BSR. We observe a clear increase in amplitudes with offsets for CDPs (572-574) with BSR, no significant increase of amplitudes with offsets for CDPs (967-969) without BSR. This shows that the sediments below the BSR contain free-gas.



**Figure 4.** The Amplitude versus offset plot for group of CDPs, (a) 572-574 (with BSR) and (b) 967-969 (without BSR) . Fig 4a shows a clear increase in amplitude with offset, while in case of Fig 4b we don't observe such marked increase.

#### SEISMIC ATTENUATION

Seismic Attenuation is the phenomenon which describes the loss of energy due to the wave propagation through the sediment and is characteristic of the formation usually measured by dimensionless quality factor  $Q$ . Seismic quality factor depends on the factors such as rock property, fluid type and degree of fluid saturation. The increase in  $Q$  indicates the presence of gas-hydrates (Gei and Carcione, 2003; Bellefluer, et al, 2007) and this increase depends on the nature of distribution and amount of hydrates within the sediments. In some cases, the presence of fluids or coexistence of gas-hydrates and free-gas within GHSZ decreases  $Q$  (Chand and Minshull, 2004; Priest et al, 2006). The increase in attenuation with increasing hydrate concentration has been observed in the Mackenzie delta (Guerin and Goldberg, 2002) and in the Nankai trough (Matshushima, 2005; 2006) against the background. However, these measurements are based on the sonic logs and are not derived from the low-frequency seismic data. The anomalously high  $Q$  with respect to the background can be used to detect gas-hydrates and this concept has

been applied successfully to the marine seismic data (Sain et al., 2009; Sain and Singh, 2011).

In time domain,  $Q$  is usually estimated by pulse amplitude decay (Brzostowski and McMechan, 1992), pulse rising time (Kjartansson, 1979), and pulse broadening (Wright and Hoy, 1981), and all of them use pulse amplitude information. Nevertheless, amplitude information of seismic pulses is often influenced by scattering, geometric spreading and other factors. In frequency domain, approaches of  $Q$  estimation include the logarithm spectral ratio (LSR) (Hauge, 1981; Raikes and White, 1984; Sain et al., 2009; Sain and Singh, 2011), centroid frequency shift (CFS) (Quan and Harris, 1997), and peak frequency shift (PFS) (Zhang and Ulrych, 2002; Gao and Yang, 2007) methods, all of which require Fourier transforms to calculate the frequency spectra of seismic records sampled within a time window. In our case, we have used the PFS method for computation of the  $Q$ -factor.

As the seismic energy travels through the earth, high frequency components are attenuated more than the low frequency components, resulting in a shift of the peak

frequency of the signal at the receiver. The amplitude of the signal also decreases and pulse broadening occurs.

We have computed the Q for CDP 504 with a BSR and for CDP 912 without any BSR to illustrate the effect of gas hydrates on seismic attenuation or quality factor. The frequency shift is pursued by performing amplitude analysis for the seafloor and for the BSR in selected time gates, and then computing the frequency spectra using Fourier transformation. The peak frequencies of seafloor

and that of BSR are plotted on the same scale (Fig.5a &b) and the frequency shift is measured. Q is computed at the same offset, i.e, at 306 m for both CDP 504 and CDP 912. The attenuation coefficients for CDP 504 and CDP 912 are calculated as 0.01016 and 0.01635, respectively. The respective quality factors are calculated as 222.51 and 148.271. The presence of BSR causes clear increase in Q-factor or reduction in attenuation and thus indicates presence of gas-hydrates above the BSR.

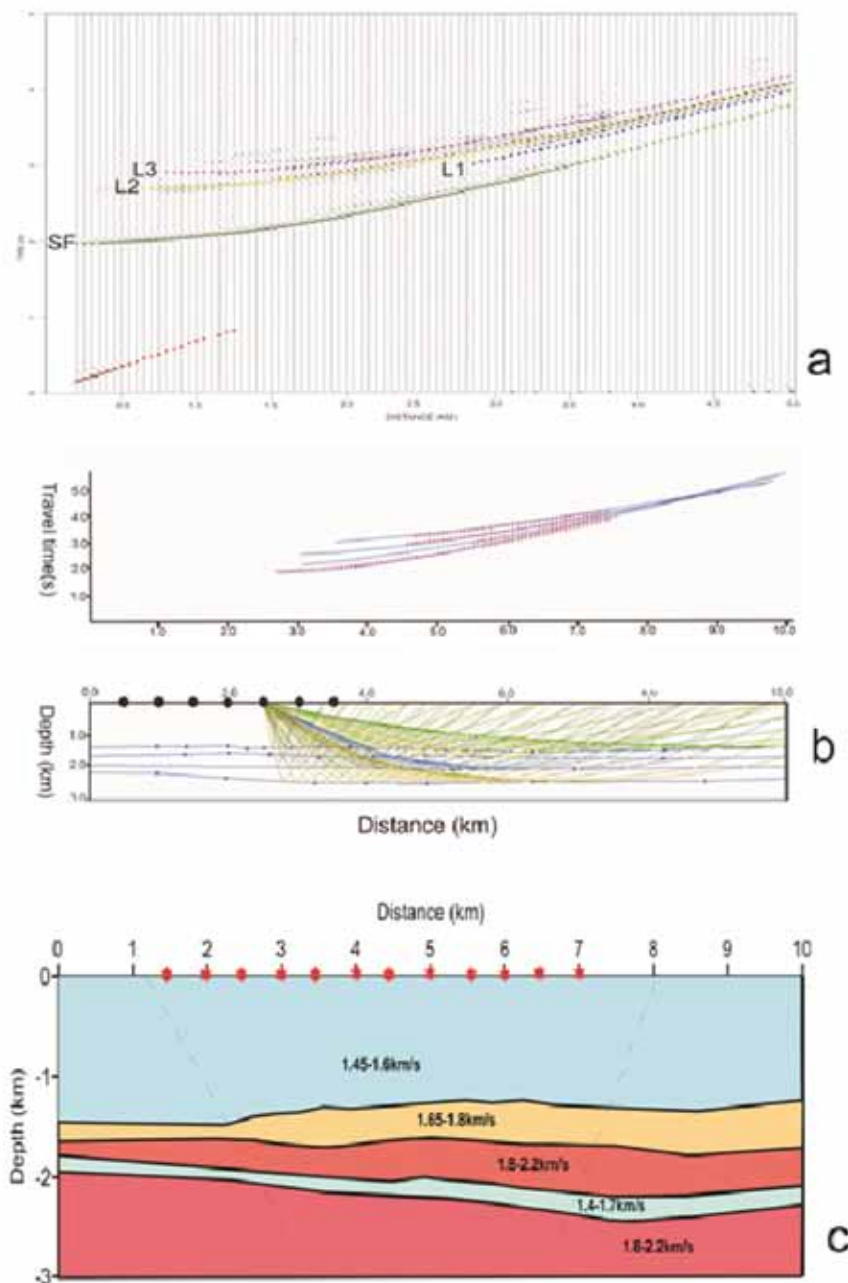


**Figure 6.** (a) The travel time picks made along four prominent reflectors shown as SF, L1, L2, L3 respectively (b) Ray-tracing model showing the fit between the observed and computed travel times. Red dots show observed travel times, while the solid blue lines are the computed travel times for each reflector and (c) The final velocity – depth model derived along the seismic profile showing the gas hydrate and free gas layer.

## VELOCITY MODELING

A scheme for the quantification of gas-hydrate reserve is mainly governed by the accurate estimation of seismic velocities. Thus, the velocities obtained by detailed velocity analysis cannot be routinely used for quantification of gas-hydrates. Reconstruction of seismic velocities along the seismic profile provides a good starting point for resource estimation and constrains the quantitative estimates of gas-hydrate volume as well as underlying free gas as a first approximation. In the context of above, it becomes imperative to adopt a technique that can give a reliable velocity structure along the seismic line. Application of tomographic technique to the MCS reflection data to reconstruct the acoustic velocity distribution has yielded some good results earlier (Tinivella, et al, 1996, 2000; Thakur et al, 2007; Singh and Sain, 2012, Satyavani and Sain, 2014) and we also have adopted the same technique here to arrive at the velocity depth structure along the seismic line.

We have constructed the velocity depth model using the travel times of correlatable reflected phases observed on shot-gathers spaced at 500 m intervals along the seismic line. The travel-time modeling is performed using the RAYINVR method of Zelt and Smith (1992). The inversion algorithm requires a starting velocity model for the subsurface, which is described by two types of model parameters, velocity nodes and boundary nodes. The latter is used to specify the depth of interface points between layers. These nodes are connected linearly to generate layers and the velocity field for each layer is defined such that it can vary linearly across upper and lower interfaces, providing a vertical velocity gradient within the layer. A total of 5 phases are picked on all the shot-gathers but only four are considered in modeling, since the phase pertaining to the diving wave (shown in red in Fig.6a) has a very limited extent. The four phases are the ones corresponding to the seafloor reflection (SF), a strong reflection below the seafloor (L1), BSR (L2) and BGR (L3) (Fig.6a). The picking of BSR was done by observing the phase reversal noticed on the shot gathers. These travel time picks for each layer are then matched with the computed travel times till a reasonably good match is achieved by means of altering the velocities and depths defined at various nodes. In other words, the changes to the velocity /depth nodes are made in such a way that the rms residual between the observed and computed travel time is limited to 0.02 s.

The velocity depth model (Fig.6c), obtained by this procedure, shows ~200 m thick low velocity zone (LVZ) with a velocity of 1.4-1.7 km/s underlain by a high velocity (1.8-2.2 km/s) layer with ~400 m thickness. The high velocity layer may be interpreted as a hydrate layer, while the LVZ underneath can be interpreted as a free-gas layer.

## RESULTS AND DISCUSSIONS

Seismic reflection data from Andaman offshore has been examined for studying the possible presence of gas hydrate/free gas occurrences based on identification of BSR. A predominant increase in amplitude is noticed at the location of BSR, which is almost double the amplitude of seafloor reflection, indicating the presence of free gas below the BSR. This inference agrees with the results from recent drilling at site 17A of Expedition-01 of Indian NGHP (Collett et al., 2008), where pressure cores have shown the evidence of gas-hydrates and methane gas.

Seismic attenuation (Q-factor) studies also have indicated the presence of gas-hydrates in shallow sediments. These studies have been carried out at two CDP locations: one with a BSR and the other without any BSR. The Q-factors, computed in the present study for two locations with and without BSR, are 222.51 and 48.27 respectively. This high Q-factor can be interpreted as due to presence of gas-hydrates, as has been demonstrated by Sain et al. (2009) in the Kerala-Konkan basin in the western Indian margin, and by Sain and Singh (2011) in the Makran accretionary prism.

The P-wave velocities, estimated by ray based modeling, show the general distribution of the gas-hydrates / free gas along the seismic line. Spectral analysis of MCS data in this region indicates that the dominant frequency is centered around 45 Hz and the frequency range from 10 to 80 Hz contributes mainly to the amplitude. The corresponding vertical resolvable thickness ( $\lambda/4$ ) (where  $\lambda$  is the spatial wavelength) with acoustic velocity 2,000 m/s for this dominant frequency is about 12 m. Under these constraints, it may not be possible to resolve layers less than 12 m. However, the layers for which the thicknesses are derived from the present exercise are all greater than this vertical resolvable limit and the results do not suffer from this drawback. The location of the NGHP-01-17A drill-hole is about 20 km away from this seismic line, and as such one-to-one correlation of depths is not possible. The free gas zone and also the gas-hydrate zone show a gradual increase in thickness from east to west. The study brings out a ~200 m free-gas zone with a velocity of 1.4-1.7 km/s below gas-hydrate-bearing sediments with velocity of 1.8-2.2 km/s and average thickness of ~ 400 m.

## ACKNOWLEDGEMENTS

We thank Director, CSIR-NGRI for his kind permission to publish this work. Directorate General of Hydrocarbons (DGH) Noida, New Delhi is acknowledged for providing the data. We also thank the anonymous reviewer for the constructive suggestions. This is a contribution to GENIAS project at NGRI under the 12<sup>th</sup> Five Year Plan of CSIR.

## REFERENCES

- Andreassen, K., Hart, P. E., and MacKay, M., 1997. Amplitude versus offset modeling of the bottom simulating reflection associated with submarine gas hydrates. *Marine Geology* v.137, pp:25-40.
- Bellefleur, G., Riedel, M., Brent, T., Wright, F. and Dallimore, S.R., 2007. Implication of seismic attenuation for gas hydrate resource characterization, Mallik, Mackenzie Delta, Canada. *J Geophys Res*, v.112, no.B10, 311.
- Brzostowski, M., and McMechan, G., 1992. 3-D tomographic imaging of near-surface seismic velocity and attenuation. *Geophysics*, v.57, pp: 396-403.
- Collett, T.S., Riedel, M., Cochran, J., Boswell, R., Presley, J., Kumar, P., Sathe, A.V., Sethi, A.K., Lall, M.V., Sibal, V.K., NGHP Expedition 01 Scientists., 2008. NGHP EXPEDITION 01 (2006), Initial Reports. Directorate General of Hydrocarbons, NOIDA and Ministry of Petroleum & Natural Gas, India, vol 4.
- Chand, S. and Minshull, T.A., 2004. The effect of hydrate content on seismic attenuation: A case study for Mallik 2L-38 well data, Mackenzie delta, Canada. *Geophys. Res. Lett.* v. 31, no.14, 609.
- Chopra, N.N., 1985. Gas Hydrate an unconventional trap in fore-arc regions of Andaman offshore. *Bulletin of O.N.G.C.* v.22, no.1.
- Ecker, C., Dvorkin, J., and Nur, A., 1998. Sediments with gas hydrates; internal structure from seismic AVO. *Geophysics*, v. 63, no.5, pp: 1659-1669.
- Gao, J. H., and Yang, S. L., 2007. On the method of quality factors estimation from zero-offset VSP data: *Chinese Journal of Geophysics (in Chinese)* v.50, no.4, pp: 1198 – 1209.
- Gei, D. and Carcione, J.M., 2003. Acoustic properties of sediments saturated with gas hydrate, free gas and water. *Geophys Pros.* v.51, pp:141-157
- Guerin, G. and Goldberg, D., 2002. Sonic waveform attenuation in gas hydrate-bearing sediments from the Mallik 2L-38 research well, Mackenzie Delta, Canada. *J Geophys Res.* v.107, pp:2088
- Hauge, P.S., 1981. Measurements of attenuation from vertical seismic profiles. *Geophysics* v. 46, no.11, pp: 1548-1558.
- Hyndman and Spence, 1992. A seismic study of methane hydrate marine bottom simulating reflectors. *J Geophys Res.*, v. 97, pp: 6683- 6698.
- Kjartansson, E., 1979. Constant Q-wave propagation and attenuation: *J. Geophys. Res.* v.84, pp: 4137-4748.
- Krishnamohan, S.G., Dangwal, V., Sengupta S. and Desai A.G., 2006. , Andaman basin – A future exploration target. *The Leading Edge* August, pp: 964-967.
- Matshushima, J., 2005., Attenuation measurements from sonic waveform logs in methane hydrate-bearing sediments at the Nankai Trough exploratory well off Tokai, central Japan. *Geophys Res Lett.* v.32, pp:L03306.
- Matshushima, J., 2006. Seismic attenuation in methane-hydrate-bearing sediments: vertical seismic profiling data from the Nankai Trough exploratory well, offshore Tokai, central Japan. *J Geophys Res.* v.111, pp:B10101.
- Priest, J.A., Best, A.I. and Clayton, C.R.I., 2006. Attenuation of seismic waves in methane gas hydrate-bearing sand. *Geophys J Int.* v.164, pp:149-159
- Quan, Y., and Harris, J.M., 1997. Seismic attenuation tomography using the frequency shift method. *Geophysics*, v.62, no.3, pp: 895-905.
- Raju, K., Ramprasad, K. A. T., Rao, P.S., Rao, B.R. and Varghese, J., 2004. New insights into the tectonic evolution of the Andaman basin Northeast Indian Ocean. *Earth and Planetary Science Letters*, v.221, pp:145-162.
- Raikes, S.A. and White, R.E., 1984, Measurements of earth attenuation from down-hole and surface seismic recordings: *Geophysical Prospecting*, v.32, pp:892-919.
- Sain, K., Singh, A.K., Thakur, N.K. and Ramesh Khanna., 2009. Seismic quality factor observations for gas-hydrate-bearing sediments on the western margin of India. *Mar Geophy Res*, v. 30, pp:137-145.
- Sain, K. and Singh, A.K., 2011. Seismic quality factors across a bottom simulating reflector in the Makran accretionary prism, *Marine and Petroleum Geology*, v.28, pp: 1838-1843.
- Satyavani, N., Sain, K., Lall, M. and Kumar, B.J. P., 2008. Seismic attribute study for gas hydrates in the Andaman Offshore India *Mar Geophys. Res.* v.29, pp: 167-175.
- Satyavani N., and Sain K., 2014. Seismic insights into bottom simulating reflection (BSR) in the Krishna Godavari basin, Eastern Margin of India. *Marine Georesources and Geotechnology*, In Press.
- Singh, P.K. and Sain, K., 2012. 2-D Velocity structure in Kerala-Konkan basin using travel time inversion of seismic data, *Jour. of Geol. Soc. of India*, v. 79, pp: 53-60.
- Tinivella, U., and Lodolo, E., 1996. The Blake Ridge bottom-simulating reflector transect: Tomographic velocity field and theoretical model to estimate methane hydrate quantities *Proceedings of the Ocean Drilling Program. Initial Report*, 164.
- Tinivella, U. and Accaino, F., 2000. Compressional velocity structure and Poisson's ratio in marine sediments with gas hydrate and free gas by inversion of reflected and refracted seismic data (South Shetland Islands, Antarctica). *Mar Geol.* v.164, pp:13-27.
- Thakur, N.K., Prasada Rao, P., Vishwanath, N., Rajput, S. and Ashalatha, B., 2007. Tomographic approach for gas hydrate investigations in Kerala-Konkan region, India. *Mar Geophys Res.* v.28, pp: 373-378.
- Wandrey, C.J., 2006, Eocene to Miocene Composite Total Petroleum System, Irrawaddy-Andaman and North Burma Geologic Provinces, Myanmar, Chapter E in Wandrey, C.J., ed., *Petroleum systems and related geologic studies in Region 8, South Asia: U.S. Geological Survey Bulletin*, v.2208-E, pp:26.

## Gas Hydrate occurrences in the Andaman offshore, India – Seismic Inferences

Wright, C. and Hoy, D., 1981, A note on pulse broadening and anelastic attenuation in near-surface rocks: *Phys. Earth Plan. Interiors*, v.25, pp:1-8.

Yuan, T., Spence, G.D., Hyndman, R.D., Minshull, T.A. and Singh, S.C., 1999. Seismic velocity studies of a gas hydrate bottom-simulating reflector on the northern Cascadia continental margin: amplitude modeling and full waveform

inversion. *J Geophys Res*, v. 104, no.1, pp: 179–1,191.

Zelt, C.A. and Smith, R.B., 1992. Seismic travel-time inversion for 2-D crustal velocity structure. *Geophys J Int.* v. 108, pp:16–34

Zhang and Ulrych., 2002. Seismic absorption compensation: A least squares inverse scheme *Geophysics* v.72, no.6, pp: R109-R114.